Glasses with ferroelectric phases

IOP Conf. Series: Materials Science and Engineering **2** (2009) 012012 doi:10.1088/1757-899X/2/1/012012

Glasses with ferroelectric phases

M.A. Valente, M.P.F. Graça

Physics Department (I3N - FSCOSD), Aveiro University, 3800-193 Aveiro, Portugal

E-mail: mav@ua.pt

Abstract. Glasses ceramics, with ferroelectric phases embedded in the glass matrix, were prepared by the melt- quenching through heat-treatments (HT) of silicate, borate and phosphate glasses. Some glasses were heat-treated with the application of an external electric field (TET). The structure and morphology of the samples were studied by X-ray powder diffraction (XRD), Raman spectroscopy and scanning electron microscopy (SEM). The dielectric properties, in function of frequency and temperature, were studied and discussed through a three serial of a resistance in parallel with a constant phase element (CPE), two related with the sample surfaces and one with the bulk material, showing that the bulk has the major contribution for the dielectrical characteristics. The temperature dependence of the dc electrical conductivity (σ_{dc}), the thermally stimulated depolarization current (TSDC), and the ac conductivity (σ_{ac}), measured at 1 kHz, were used to characterize the samples. The structure, the dielectric properties and the electrical conductivity reflect the important role carried out by the base glass the heat-treatment and the electric field during the HT and the ferroelectric phases in the properties of glass–ceramics.

1. Introdution

Lithium niobate ($LiNbO_3$), is an important material due to its excellent pyroelectrical, piezoelectrical, photorefractive properties and optoelectronic applications. It is used for active waveguides, modulators, frequency doubler, optical filter, Q-switches and in integrated optical circuits [1-8]. Potassium niobate ($KNbO_3$), is a nonlinear optical material with second harmonic generation, photorefractive, piezoelectric electro and acousto-optic properties. $KNbO_3$ crystals are used as optical waveguides, frequency doublers, holographic storage systems, nonvolatile ferroelectric memories, dielectrics and wireless communication. This crystal undergoes phase transitions, with the rise of the temperature (rhombohedral→orthorhombic→tetragonal→cubic). In the last transition, the crystal looses its ferroelectric properties [9]. Sodium niobate ($NaNbO_3$) has antiferroelectric properties under ambient conditions and presents an unusually large number of phase transitions. On cooling from the high-temperature paraelectric phase, it undergoes to antiferroelectric and to ferroelectric phase at temperatures below 170K. The $NaNbO_3$ is a material that shows a good combination of electrical, mechanical and chemical properties [10-12]. The preparation of ferroelectric crystals, is difficult, time consuming and very expensive. The glass-ceramic processing, with the temperature, atmosphere and time as parameters, seems to be an alternative, to the sintered ceramics and single crystals preparation, for getting dense materials, with ferroelectric phases, due to its relative low preparation time and costs and the ability to: avoid the coarsening and aggregation of crystalline particles; control the shape, size and distribution of the crystalline phase and their properties.

2. Experimental

Silicate, borate and phosphate glasses were prepared by the melt-quenching technique. The as-prepared glass has been HT in air without and with the application of an electric field (TET). The structure and morphology of the samples were studied by XRD, Raman spectroscopy and SEM microscopy. The dc electrical conductivity, σdc, and the thermally stimulated depolarization current (TSDC) was measured as a function of the temperature from 100K to 400K. The ac conductivity (σac) measurements, carried out between 80K and 370 K, were obtained by measuring the sample capacitance (C) and conductance (G). The impedance spectroscopy measurements ($Z^* = Z' - jZ''$) were carried out as a function of the temperature (200 K–300 K), in the frequency range of 10 Hz –32 MHz.

3. Results

In the present work we will present some representative results of the prepared samples. A more complete discussion is made in the previous articles published by us [1-14]. Figure 1 shows the macroscopic aspect of the silicate glasses TET. The presence of an external electric field during the HT, leads to the formation of a white layer in the surface in contact with the positive electrode. This layer was not observed in the sample surface in contact with the negative electrode.

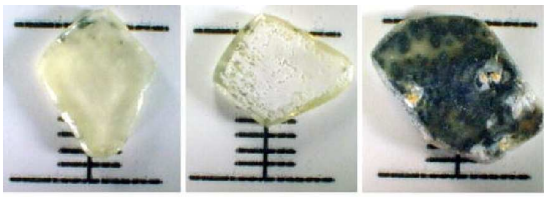

Figure 1. Photograph of the $60SiO_2$-$30Li_2O$-$10Nb_2O_5$ (%mole) glass samples surfaces after TET: i- in contact with the negative electrode; ii- in contact with the positive electrode; iii—the 500 kV/m TET sample at 600 °C [6].

The $LiNbO_3$ phase was detected by XRD in the 650 °C HT and in the 600 °C TET samples. However, particles were observed, by SEM in the transparent 600HT sample, but not detected by XRD, an indication of the amorphous or incipient crystallization of these particles. Figure 2 shows SEM micrographs of glass with lithium of the system: (a) silicate (HT, 600ºC); (b) borate (HT, 450HT) and (c) phosphate (HT, 450ºC). The rise of the HT temperature increases the amount of the particles present in the samples. The TET promotes the formation in the surface cathode of a 40–60 μm layer and in the surface anode a visible white layer (50-100 μm). These layers, suggests the existence of an oxidation–reduction reaction in the samples surface, activated by the electric field. The region near the anode presents a higher number of particles when compared with the cathode side. The size of these particles increases with the rise of the applied electric field. In the cross section of these TET samples the particles number increases, with the rise of the applied electric field.

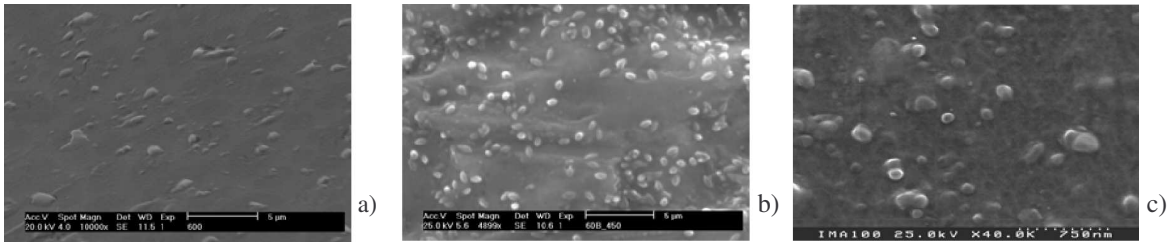

Figure 2. SEM micrographs of glass with lithium of the system: (a) silicate, HT at 600ºC; (b) borate, HT at 450HT and (c) phosphate, HT at 450ºC.

Figure 3 shows the XRD patterns of the niobate glasses with lithium (Figure 3a) and with sodium and potassium (Figure 3b). In these spectra we present the silicate, borate and phosphate glass compositions. The $LiNbO_3$ phase was obtained in all glass systems. The XRD peaks not indexed in the figures are associated with secondary phases.

In all system the σ_{dc} decreases with the increase of the HT temperature and with the rise of the amplitude of the applied electric field in the TET (Figure 4a). At 300K, the σ_{dc} normally decreases with the increasing of the HT temperature. The temperature dependence of the σ_{dc} can be adjusted by the Arrhenius formalism (represented inside Figure 4a) and the activation energy $E_{a(dc)}$ calculated. For some samples, the Arrhenius model reveals that, at least, two activation energies exist in the measuring temperature range. Figure 4b shows the ac conductivity (σ_{ac}) temperature dependence of the $44SiO_2$-$33Li_2O$-$23Nb_2O_5$ (%mole) as-prepared sample, for some frequencies of measurement. It is observed that the increase of the frequency leads to an increase in the σ_{ac} ($\sigma_{ac} = \omega\varepsilon_0\varepsilon''$, where ω represents the angular frequency, ε_0 the permittivity of the empty space and ε'' the imaginary part of the sample complex permittivity (ε^*)) and to a decrease of the $E_{a(ac)}$. This behaviour is the same for all the samples.

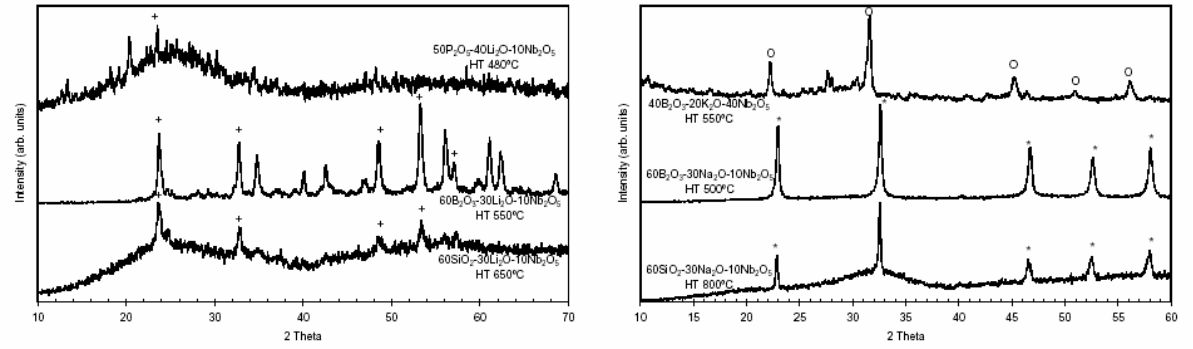

Figure 3. XRD patterns of different glass systems, represented in molar composition. (+ $LiNbO_3$; * $NaNbO_3$; O $KNbO_3$)

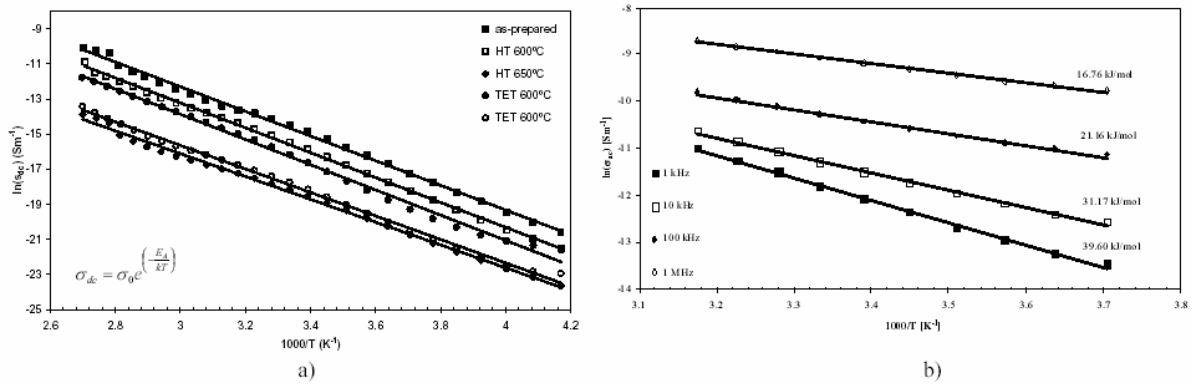

a) b)

Figure 4. a) The σ_{dc} temperature dependence of the $60SiO_2$-$30Li_2O$-$10Nb_2O_5$ (mole %) glasses; b) The σ_{ac} temperature dependence of the $44SiO_2$-$33Li_2O$-$23Nb_2O_5$ (mole %) glasses, for several frequencies [6].

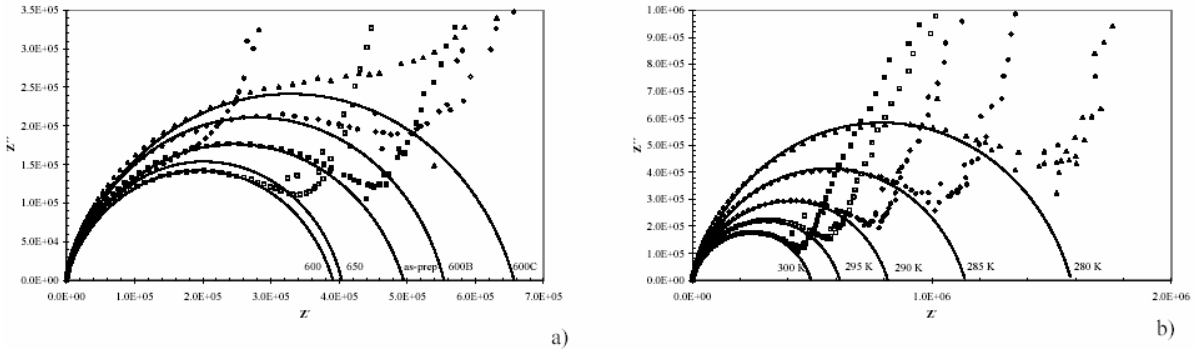

Figure 5. The Z′ vs. Z″ plot of: a) $60SiO_2$-$30Li_2O$-$10Nb_2O_5$ (%mole) glass, treated at different temperatures and measured at 300K b) the as-prepared sample, at different measured temperatures. The lines are the theoretical adjust [5].

Figure 5 shows the Z' vs. Z'' of all the samples $60SiO_2$-$30Li_2O$-$10Nb_2O_5$ (normalized, by $Z^*=Z^*_{measured}(A/d)$ - A is the electrode area; d the sample thickness). A quantitative characterization of the Z^* has been made using a complex nonlinear least squares algorithm (CNLLS), which revealed that a resistance (R) in parallel with a CPE element equivalent circuit fits the impedance data. For all the samples, with the rise of the measurement temperature the R parameter decreases, the Q_0 increases and the n remain, approximately, constant. The dielectric constant (ε' – obtained through $Z^* = 1/(\mu\varepsilon^*)$) at 1 kHz and 300 K, increases with the rise of the HT temperature. The TET samples present a ε' values similar to that of the as-prepared sample. The mean value of the relaxation time distribution, τ_Z ($\tau_Z = 1/\omega_Z$), observed with the impedance formalism, increases with the rise of the amplitude of the applied field, and decreases with the increase of the measurement temperature.

Figures 6 present the TSDC spectra of the $60SiO_2$-$30Li_2O$-$10Nb_2O_5$ treated at 650ºC. All samples present, in the temperature measuring range used, two TSDC peaks. These peaks were fitted using the following equation (Eq.1), and the results are showed by the lines in the spectra (Figure 6).

$$i(T) = A \exp\left(-\frac{E_a}{k_B T}\right) \exp\left[-B \int_{T_0}^{T} \exp\left(-\frac{E_a}{k_B T'}\right) dT'\right] \qquad (1)$$

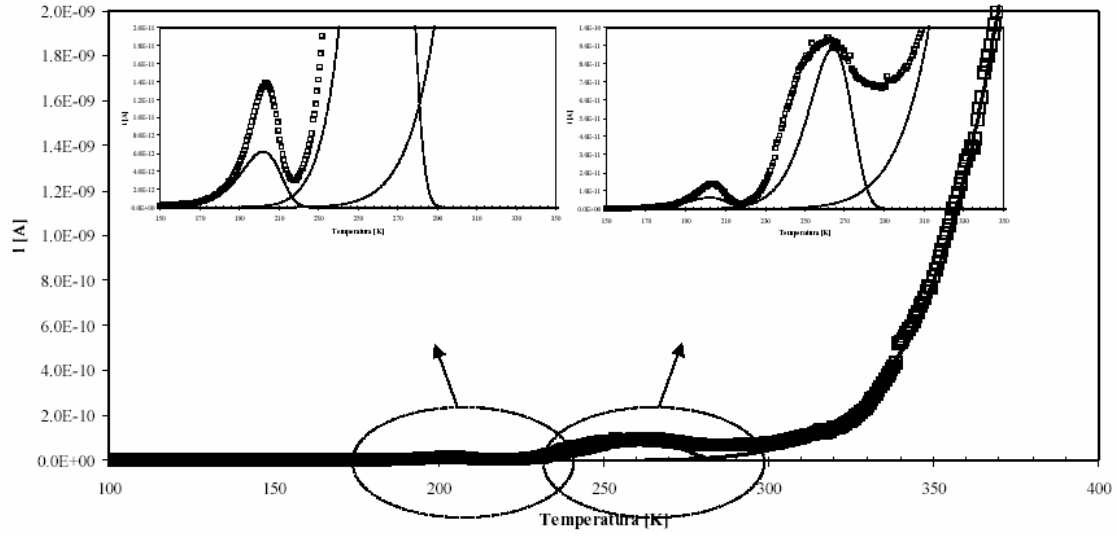

Figure 6. TSDC current in function of the measuring temperature for the glass $60SiO_2$-$30Li_2O$-$10Nb_2O_5$ (%mole) treated at 650ºC. The lines are the theoretical adjust.

4. Discussion

The decrease of the dc conductivity (σ_{dc}) with the rise of the HT temperature can be assigned to the decrease of the number of network modifiers and consequent increase of the volume ratio between the crystalline phases and the glass matrix. It should be noticed that in the studied glasses, was detected, by Raman spectroscopy, the presence of niobium ions inserted in the glass matrix as network modifiers. The observed decrease of the $E_{a(dc)}$, with the rise of the HT temperature was associated to a decrease in the height of the free energy barriers of the glass matrix quasi-lattice making the jump process easier and contributing to a higher mobility. This indicates that the charge carriers number, although diminishing in number with the increase of the HT temperature, dominate this conduction process. In all samples, the observed increased of σ_{dc} with the rise of the measurement temperature, characteristic of a thermally stimulated process, indicates an increase of the charge carriers energy, with the increase of the temperature.

The σ_{ac} behavior can be explained through the hopping motion of the ions. The decrease of the σ_{ac} should be assigned to the decrease of the free ions number and to the increase in the amount of crystalline phases, whose dipoles are difficult to depolarize. The small fluctuations of the $E_{a(ac)}$, with the increase of the HT temperature, suggest that this physical parameter is dominated by the glass matrix rather than by the free ions number or the crystallites electrical characteristics.

In the TET samples the decrease of both σ_{dc} and σ_{ac}, with the rise of the applied field, should be associated with the increase in the size and number of the crystalline phases, and the decrease in the free ions number. The TET samples show three different zones: the surfaces and the inside zone. It must be pointed out that in these samples, the anode surface (containing a white opaque coat) presents a higher number of crystalline particles than the cathode surface and that of the bulk, which has a reduced number of particles. For the dielectrical analysis, these zones can be associated to three serial capacitors model: two related with the sample surfaces and one with the bulk material. If we assume that the capacity of the surfaces, related with the dielectric constant (ε') of $LiNbO_3$, is larger than the capacity of the bulk material, it becomes reasonable to consider that the bulk material has the higher contribution for the dielectric behavior. Thus, the values of the ε' in the TET samples, that are similar to that of the as-prepared sample, are over all due to the bulk material.

In the HT samples the increase of ε', with the rise of the heat treatment temperature, can be assigned to the increase of the volume ratio between the ferroelectric phases and the glass matrix.

From the Z' vs. Z'' plot, the observed semi-arcs, which centers are under the Z' axes, indicate the existence of a distribution of relaxation times. This behavior can be associated with the dielectric responses of the glass matrix, the ferroelectric phase and other dipoles arising from the free electric units. All the samples present a low-frequency Warburg response type, which can be attributed to the sample/electrode interface dipoles. The theoretical fit of the Z^* data revealed that a resistance (R) in parallel with a constant phase element (CPE) is an equivalent circuit that can describe the measured data. In the TET samples the increase of the R-parameter, with the rise of the applied field should be associated with the increase of the volume ratio between the crystalline phases and the glass matrix. The observed increase of τ_Z , is another indication of this raise, because the ferroelectric dipoles are difficult to depolarize at room temperature. In all samples, the R-value, decreases, with the rise of the measurement temperature, which is in agreement with the σ_{dc} and σ_{ac} temperature dependence, indicating that the raise of the temperature lead to an increase in the energy, and consequent mobility of the charge carriers. This assumption is also supported by the decrease of τ_Z, with the rise of the measurement temperature, which shows an increase in the ability of the dielectric units in following the ac field.

The TSDC peak at lower temperatures is assigned to movements of the ions inserted structurally in the glass matrix. The second peak, at higher temperatures, was attributed to space-charge polarization resulting from the movements of the charge carriers in limited paths that are due to the presence of micro-heterogeneities. After the second peak, the increase of the depolarization current with the

increase of the measuring temperature can be related to a surface-electrode polarization phenomenon. The TSDC theoretical fit indicates the existence of a larger number of relaxation processes. Thus the TSDC data must be described assuming the existence of a relaxation time distribution.

5. Conclusions

The ferroelectric crystallites were detected in samples heat-treated above 500°C-600ºC. The presence of two different dc activation energies indicates the existence of two different activated mechanisms. The decrease of the σ_{ac}, with the rise of the HT temperature, was attributed to the decrease of the electrical units number (ions/dipoles) or to an increase of their movement difficulty. The Raman spectroscopy indicates that niobium ions are inserted in the glass matrix as network modifiers. The electrical conduction process is dominated by the charge carriers number. The increase of ε' and of τ_Z, with the rise of the HT temperature, was assigned to the increase of the volume ratio between the crystalline phases and the glass matrix. In the TET samples the ε' behavior was assigned to the bulk material characteristics. The dielectric theoretical fit reveals that a resistance in parallel with a CPE element is an equivalent circuit to describe the measured data. The TSDC results show the presence of current peaks assigned to: - P1 (low temperature peak): local movements of free ions in the glass network between positions around the non-bridging oxygen (NBO) to which is bonded; - P2 (second peak peak): dipole depolarization from the charge carriers movements in limited paths, resulting from glass micro-heterogeneities and giving origin to space–charge polarization. For higher temperatures, an electrode-sample interfacial polarization phenomenon is detected.

References

[1] Graça M P F, Silva M G F and Valente M A 2002 *Adv. Materials Forum I*, **230-232** 161-64.
[2] Graça M P F, Valente M A and Silva M G F 2003 *J. Non-Cryst. Solids* **325- 1-3** 267-74.
[3] Graça M P F, Silva M G F and Valente M A 2005 *J. Non-Cryst. Solids* **351** 2951-57.
[4] Graça M P F, Valente M A and Silva M G F 2006 *J. Mat. Science* **41** 1137-44.
[5] Graça M P F, Silva M G F, Sombra A S B and Valente M A 2006 *J.Non-Cryst. Solids* **352** 5199-5204.
[6] Graça M P F, Silva M G F, Sombra A S B and Valente M A 2007 *J. Mat. Science* **42 (8)** 2543-2550.
[7] Graça M P F, Silva M G F, Sombra A S B and Valente M A 2007 *J. Non- Cryst. Solids* **353** 4390-4394.
[8] Graça M P F, Silva M G F and Valente M A 2008 *J. Non-Cryst. Solids* **354** 901-908.
[9] Graça M P F, Silva M G F and Valente M A 2008 *J. Eur. Cer. Society* **28** 1197-1203.
[10] Graça M P F, Silva M G F, Sombra A S B and Valente M A 2008 *J. Non-Cryst. Solids* **354 29** 3408-13.
[11] Figueira R C C, Graça M P F, LC Costa and Valente M A 2008 *J. Non-Cryst. Solids* **354** 47-51 5162-64.
[12] Graça M P F, Silva M G F and Valente M A 2006 *Adv. Materials Forum III,* PTS 1-2, **514-516** 274-279.
[13] Graça M P F, Silva M G F, Sombra A S B and Valente M A 2007 *Physica B* **396** 62-69.
[14] Graça M P F, Silva M G F and Valente M A 2009 *Solid State Sciences* **11** 570-577.